Global Hairpin Folding of Tau in Solution†

Sadasivam Jeganathan,‡,§ Martin von Bergen,*,‡,§ Henrik Brutlach,|| Heinz-Jürgen Steinhoff,|| and Eckhard Mandelkow*,‡

Max Planck Unit for Structural Molecular Biology, Notkestrasse 85, D-22607 Hamburg, Germany, and Department of Physics, University of Osnabruck, D-49069 Osnabruck, Germany

Received October 21, 2005; Revised Manuscript Received December 20, 2005

ABSTRACT: The microtubule-associated protein tau stabilizes microtubules in its physiological role, whereas it forms insoluble aggregates (paired helical filaments) in Alzheimer's disease. Soluble tau is considered a natively unfolded protein whose residual folding and intramolecular interactions are largely undetermined. In this study, we have applied fluorescence resonance energy transfer (FRET) and electron paramagnetic resonance (EPR) to examine the proximity and flexibility of tau domains and the global folding. FRET pairs spanning the tau molecule were created by inserting tryptophans (donor) and cysteines (labeled with IAEDANS as an acceptor) by site-directed mutagenesis. The observed FRET distances were significantly different from those expected for a random coil. Notably, the C-terminal end of tau folds over into the vicinity of the microtubule-binding repeat domain, the N-terminus remains outside the FRET distance of the repeat domain, yet both ends of the molecule approach one another. The interactions between the domains were obliterated by denaturation in GdnHCl. Paramagnetic spin-labels attached in various domains of tau were analyzed by EPR and exhibited a high mobility throughout. The data indicate that tau retains some global folding even in its "natively unfolded" state, combined with the high flexibility of the chain.

Tau protein is prominent in neurons and plays an important role in neurite outgrowth and axonal transport by stabilizing microtubules which provide the tracks for motor proteins. Tau is a highly soluble protein due to its hydrophilic character, yet it aggregates into insoluble fibers (PHFs)[1] in Alzheimer's disease and other tauopathies (*1*−*3*). In solution, tau behaves largely as a random coil, as judged by electron microscopy, X-ray diffraction, CD, FTIR, fluorescence spectroscopy, NMR spectroscopy, and other methods (*4*−*8*).

Tau can be subdivided into several domains (Figure 1). The ∼120 N-terminal residues are mostly acidic and project away from the microtubule surface (*9*). The remainder of the protein has a basic character, complementary to the acidic surface of microtubules. The repeats (three or four, distinguishing the class of isoform) in the C-terminal half form the core of the microtubule-binding domain; together with the proline-rich flanking domains (*10*−*12*), they regulate growth rates and dynamics of microtubules (*13*). PHFs from Alzheimer's disease brain contain a pronase-resistant core that coincides mostly with the repeats of tau (*14*, *15*). Consistent with this, the repeat domain polymerizes in vitro with higher efficiency than full-length isoforms of tau (*5*, *16*). This abnormal aggregation is driven by a transition from random coil to β-structure in the repeat domain, based on the interaction of certain hexapeptide motifs in repeats R2

FIGURE 1: Proteins and mutations. A set of single tryptophan/cysteine mutants were created on the basis of three different isoforms of tau, htau40 (4R/2N), htau39 (3R/2N), and htau23 (3R/0N), the shortest isoforms (top). The positions of the inserted tryptophans are indicated by filled circles, and the positions of IAEDANS (labeled to cysteine) are indicated by empty circles. The FRET pairs created within tau protein and their positions are shown by bars in the bottom part of the figure.

† This project was supported in part by a grant from the Deutsche Forschungsgemeinschaft.

* To whom correspondence should be addressed. Telephone: +49-40-89982810. Fax: +49-40-89716822. E-mail: vbergen@mpasmb.desy.de or mand@mpasmb.desy.de.

‡ Max Planck Unit for Structural Molecular Biology.

§ These authors contributed equally to this work.

|| University of Osnabruck.

[1] Abbreviations: AD, Alzheimer's disease; CD, circular dichroism; $CHCl_3$, chloroform; DMF, *N*,*N*-dimethylformamide; DTT, dithiothreitol; EPR, electron paramagnetic resonance; FPLC, fast performance liquid chromatography; FRET, fluorescence resonance energy transfer; FTIR, Fourier transform infrared; GdnHCl, guanidine hydrochloride; HPLC, high-pressure liquid chromatography; IAEDANS or 1,5-IAEDANS, 5-({[(2-iodoacetyl)amino]ethyl}amino)naphthalene-1-sulfonic acid; JAA6, iodoacetamide spin-label; MTBR, microtubule binding repeat domain; PBS, phosphate-buffered saline; PHF, paired helical filament; TEMPO, 2,2,6,6-tetramethylpiperidine-1-oxyl radical.

10.1021/bi0521543 CCC: $33.50
Published on Web 01/28/2006

and R3 (*17*, *18*). For the situation in vivo, it has been suggested that apoptotic caspases cleave tau at the N-terminal and C-terminal ends, thus making it more prone to aggregation. The truncations of tau at the C-terminus (E391) by unidentified proteases (*19*) and at D421 by members of the caspase family (*20*, *21*) have been shown to increase the rate of polymerization in the presence of polyanions (heparin, RNA, and acidic peptides) (*22*, *23*) and with arachidonic acid micelles (*24*, *25*). Therefore, it has been proposed that the carboxy-terminal tail of tau acts by inhibiting its polymerization through an interaction with the repeat domain (*25*).

The N-terminal projection domain is thought to be involved in the spacing of microtubules since the knockout of the tau gene results in altered microtubule organization in small caliber axons in mice (*26*). Another hypothesis is that this domain acts as an anchor for other cell components such as kinases, phosphatases, or the plasma membrane (*27*−*29*). The role of the N-terminal domain in PHF aggregation is not well understood; it is inhibitory in the presence of heparin (*23*) but facilitates polymerization in the presence of fatty acid micelles (*30*). The reactivities of antibodies that detect an early conformational change of tau in AD (e.g., Alz-50, MC1, and Tau-66) suggest that the N-terminal end can fold over the repeat domain before polymerization (*31*, *32*). This would be consistent with an electrostatic interaction since the N-terminal domain and the repeats have opposite net charges.

To study the conformation of tau in solution, we mapped intramolecular distances by using fluorescence resonance energy transfer (FRET). For this purpose, we created a series of tau mutants containing a single tryptophan and a single cysteine, which was labeled with IAEDANS. FRET results show that the tau molecule adopts a global folding which brings the N-terminus near the C-terminus, and the C-terminus and the repeat domain close together ("paperclip fold"). Despite this folding, the mobility of the chain remains high throughout, as judged by EPR of spin-labels distributed along the molecule.

MATERIALS AND METHODS

Chemicals and Proteins. 1,5-IAEDANS was obtained from Molecular Probes (Eugene, OR), and 4-(2-iodoacetamido)-TEMPO was obtained from Sigma (Munich, Germany). Mutations were created by site-directed mutagenesis using the Quick Change kit (Stratagene, La Jolla, CA) and the plasmid pNG2. Plasmids were sequenced on both strands to confirm the mutations. Full-length tau isoforms htau40 (4R/2N), htau39 (3R/2N), htau23 (3R/0N) and their mutants (Figure 1) were expressed in *Escherichia coli* (*33*) and purified by making use of FPLC MonoS (Amersham Bioscience, Freiburg, Germany) chromatography as described previously (*11*) with minor modifications. Briefly, the cell lysate was precipitated with 25% $(NH)_2SO_4$ and centrifuged for 45 min at 127000*g*. The supernatant was adjusted to 55% saturated $(NH)_2SO_4$, and after centrifugation for 45 min at 127000*g*, the pellet was dissolved in MonoS A buffer and dialyzed against MonoS A buffer overnight. Further purification was performed as described previously (*11*). The purity of the proteins was analyzed by SDS−PAGE.

Labeling of Proteins. Protein in PBS buffer (∼100 μM) was incubated with a 10-fold molar excess of DTT for 10 min at 37 °C. DTT was then removed by size exclusion chromatography (Fast Desalting column, Amersham Bioscience), and the eluted protein was immediately added with an ∼20-fold molar excess of IAEDANS (dissolved in DMF) for FRET studies or TEMPO (dissolved in $CHCl_3$) for EPR studies. The labeling reaction was allowed to proceed overnight at 4 °C. The reaction mixture was dialyzed against PBS, and residual IAEDANS was then removed by size exclusion chromatography. The concentration of the protein was determined by absorption at 280 nm using a molar extinction coefficient ϵ_{tau} of 10800−12100 M^{-1} cm^{-1}, depending on the different contents of aromatic residues in the isoforms and mutants of tau. The amount of bound IAEDANS was determined by the absorption at 336 nm ($\epsilon_{IAEDANS} = 6100$ M^{-1} cm^{-1}) (*34*). The protein concentration was corrected for the contribution of IAEDANS at 280 nm, and the stoichiometry was calculated; typically, the labeling stoichiometry was 0.8−0.9.

Fluorescence Spectroscopy. All steady-state fluorescence measurements were performed with a Spex Fluoromax spectrophotometer (Polytec, Waldbronn, Germany), using 3 mm × 3 mm quartz microcuvettes from Hellma (Mühlheim, Germany) with a sample volume of 20 μL. Tryptophan was excited at 290 nm to prevent a contribution of tyrosine emission; scans ranged from 300 to 550 nm. In all cases, the experimental parameters were as follows: excitation slit width of 4 nm, emission slit width of 6 nm, integration time of 0.25 s, and photomultiplier voltage of 950 V. The FRET efficiency was measured by the energy transfer

$$E_{FRET} = (1 - D_A/D)(1/f_A) \quad (1)$$

where D_A is the fluorescence intensity of the donor in the presence of the acceptor and D is the fluorescence intensity of the donor in the absence of the acceptor. The apparent efficiencies were normalized by f_A, the fractional labeling with acceptor, as shown in eq 1 (*35*). The distance R between the donor and acceptor was calculated by the Förster equation

$$E_{FRET} = [1 + (R/R_o)^6]^{-1} \quad (2)$$

where the Förster radius R_o is 22 Å for the Trp-IAEDANS pair (*36*, *37*). In denaturation experiments with GdnHCl, the efficiency was calculated from emission intensities of labeled protein and unlabeled protein at the same GdnHCl concentration. The influence of various GdnHCl concentrations on the fluorimetric properties of tryptophan and IAEDANS was controlled with free dyes alone and in combination. The effects due to GdnHCl as a solvent were minor (<10%) in comparison to the FRET effects, and the spectra were corrected for it.

CD Spectroscopy. All measurements were carried out with a Jasco J-715 CD spectrometer (Jasco, Gross-Umstadt, Germany) in a cuvette with a path length of 0.01 cm. The spectra were recorded between 190 and 260 nm at a scanning speed of 100 nm/min, a bandwidth of 1.0 nm, and a response time of 2 s. In each experiment, three spectra were summed and averaged. For calculation of the mean residue ellipticity, the protein concentration was obtained by using the second channel of the CD spectrometer to measure the absorption of the protein sample at 214 nm (where absorption is

dominated by the peptide bonds). Calibration at 214 nm was done with a BSA standard.

Microtubule Polymerization Assay. Microtubule assembly was monitored by UV light scattering at an angle of 90° at a wavelength of 350 nm in a quartz cuvette (path length of 0.15 cm) in a Kontron spectrophotometer (Kontron Instruments) in the presence or absence of tau. Tau (5 μM) was mixed with 30 μM tubulin dimer at 4 °C in microtubule assembly buffer [100 mM Na-PIPES (pH 6.9), 1 mM EGTA, 1 mM $MgSO_4$, 1 mM GTP, and 1 mM DTT] in a final volume of 20 μL. The reaction was started by increasing the temperature to 37 °C.

Electron Paramagnetic Resonance Spectroscopy. A custom-built X-band EPR spectrometer equipped with a dielectric cavity (Bruker BioSpin GmbH, Rheinstetten, Germany) was used to measure EPR spectra from samples loaded in quartz capillaries. The measurements were performed at 20.5 °C and a tau concentration of ~100 μM. All experiments were performed with a modulation frequency of 50 kHz and a modulation amplitude of 0.08 or 0.16 mT. Since corresponding spectra revealed the same line widths for both modulation amplitudes, overmodulation could be excluded in the case of the 0.16 mT modulation amplitude. Depending on the EPR signal intensity, spectra were obtained by averaging of up to 60 B-field scans. The background signal originating from the sample capillaries was subtracted. The resulting standard errors and their Gaussian propagation values yielded error bars as shown in the figures.

Size Exclusion Chromatography. A set of standard proteins and tau isoforms and constructs were analyzed by size exclusion chromatography using a Superose PC12 column (Amersham Bioscience) connected to a SMART-HPLC system (Amersham Bioscience). The isocratic elution at a flow rate of 20 μL/min was performed with PBS or PBS containing 2 M GdnHCl, and the elution of the proteins was detected by UV absorbance at 214, 256, and 280 nm.

RESULTS

Proteins and Mutations. Tau as a natively unfolded protein does not contain a significant amount of secondary structure. However, even unfolded proteins are likely to contain residual secondary structure elements (*38*), and there might be some global conformation defined by interactions between the different domains of tau that would not be detectable by the usual spectroscopic methods such as CD or FTIR. To examine such interactions, we created a series of recombinant tau mutants containing a single tryptophan (donor) and a single cysteine labeled with IAEDANS (acceptor), and this allowed us to perform FRET analysis between different domains of tau (W-IAEDANS pairs, Figure 1). The mutants were created mostly on the basis of htau40 (the longest isoform in the central nervous system with four repeats and two N-terminal inserts, 4R/2N) (*39*) and also htau39 (3R/2N) and htau23 (3R/0N). As tau contains no intrinsic tryptophan, we chose conservative exchanges at hydrophobic amino acids (Y18W, Y310W, and V432W) for inserting tryptophans and exchanges at polar amino acids (T17C, S433C, and S435C) for cysteine mutation with the aim of minimizing perturbations of the protein structure. In some mutants, the naturally occurring cysteines in tau (either C291 in R2 or C322 in R3, the other one being inactivated by exchange with Ala) were used for IAEDANS labeling.

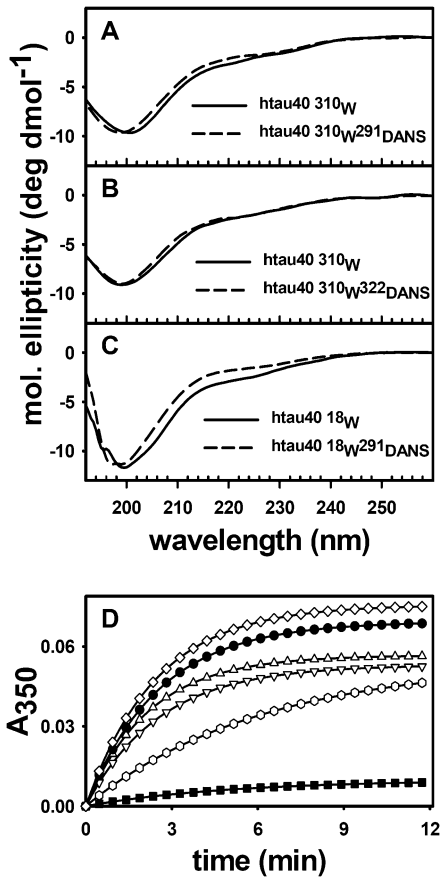

FIGURE 2: Circular dichroism spectroscopy of unlabeled and labeled proteins. The molar ellipticities of three representative examples are shown (A−C). Data for the unlabeled protein are represented by the solid line and data for the labeled protein by the dashed line. All spectra exhibit a minimum at ~200 nm, indicating a mostly random coil structure. Representative experiments of tau-induced microtubule assembly are shown in panel D. The polymerization was monitored by 90° light scattering at 350 nm. In the absence of tau (■), there is nearly no increase in the absorbance, whereas the microtubules polymerize rapidly in the presence of wild-type htau40 (●) as seen by increased absorbance. Unlabeled and labeled mutants show a similar effect on microtubule assembly comparable to that of htau40wt [htau40-310_W433_C (△) htau40-310_W322_{DANS} (⬡), htau40-310_W433_{DANS} (▽), and htau40-432_W17_{DANS} (◇)].

CD Spectroscopy and Microtubule Assembly Competence of Labeled Tau. To confirm that neither the mutations nor the labeling caused a change in the protein structure and functionality, we performed CD spectroscopy and microtubule assembly experiments (Figure 2). The CD spectra of the unlabeled mutants all exhibited a minimum at ~200 nm, indicating a mostly random coil structure which was similar to the spectra obtained for the wild-type protein (data not shown). The same was true for the labeled proteins, indicating that neither the insertion of tryptophan nor the labeling with IAEDANS had an impact on the overall secondary structure of the protein as seen by CD (Figure 2A−C). We note, however, that CD is sensitive to short-range interactions (β-sheet, α-helix), and therefore, the CD spectra do not report on global vicinities between domains. To test the effect of the mutations in terms of tau's function, we performed microtubule assembly experiments in the presence and absence of the tau mutants, both with and without the IAEDANS label (Figure 2D). Tubulin below the critical concentration remained unpolymerized, but in the presence of tau, it polymerized rapidly. Wild-type, unlabeled mutant,

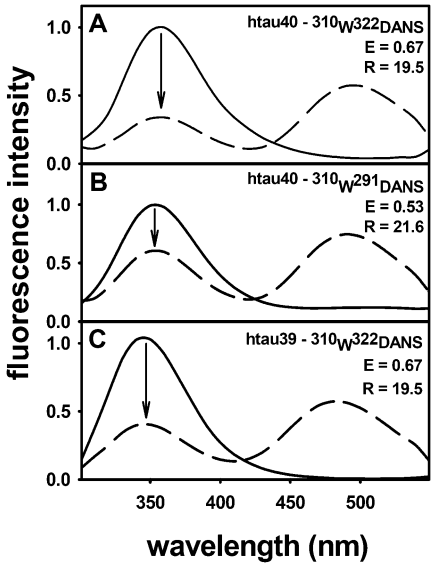

FIGURE 3: FRET within the repeat domain. The fluorescence emission spectra are shown for htau40-310_W322_{DANS} (A), htau40-310_W291_{DANS} (B), and for htau39-310_W322_{DANS} (C). The protein concentration was 2 μM; the proteins were excited at 290 nm, and the emission was recorded from 300 to 550 nm. Data for unlabeled proteins are represented by solid lines and data for labeled proteins by dashed lines. Note the strong decrease in the intensity at 350 nm due to FRET (arrow).

and labeled proteins promoted microtubule assembly with similar efficiencies, and these results fit nicely to earlier studies (*40*, *41*).

FRET Analysis within the Repeats Shows Residual Folding. To measure the distance within the repeat domain, we used mutants of htau40 and htau39 whose FRET pairs are Y310W and either C291 or C322 labeled with IAEDANS. For the unlabeled mutant, htau40-310_W322_C (single cysteine at position 322) when excited at 290 nm (Figure 3A, solid line) exhibited the typical tryptophan fluorescence with an emission maximum at 352 nm, indicating that residue 310 is almost completely solvent exposed (*40*, *42*). After C322 was labeled with IAEDANS (htau40-310_W322_{DANS}), excitation at 290 nm resulted in an additional emission peak at 490 nm (Figure 3A, dashed line), and concomitantly, the tryptophan fluorescence was strongly decreased by ~67%, although protein concentrations (2 μM) were identical. The efficiency was calculated as described in Materials and Methods and yielded an E of 0.67. Since the Förster radius for the FRET pair of tryptophan and IAEDANS is 22 Å (*36*, *37*), the FRET efficiency of 0.67 translates into a donor−acceptor distance of 19.5 Å. In the case of htau40-310_W291_{DANS}, FRET was less pronounced ($E = 0.53$, Figure 3B) than for htau40-310_W322_{DANS}, resulting in a distance of 21.6 Å. The mutant htau39-310_W322_{DANS}, based on the three-repeat isoform htau39, exhibited the same efficiency ($E = 0.67$, Figure 3C) as the corresponding mutant based on a four-repeat isoform ($E = 0.67$, Figure 3A). These results show that a strong or medium FRET can be measured between W310 near the beginning of the third repeat and C322 or C291 near the middle of repeats R2 and R3.

These calculated distances can be compared with expectations based on a model of random coil structure. The mean end-to-end distance L_m within a Gaussian coil of N amino acids can be estimated as $L_m = L_0\sqrt{N}$, where the prefactor L_0 (~8.3 Å) accounts for the stiffness of the molecule for

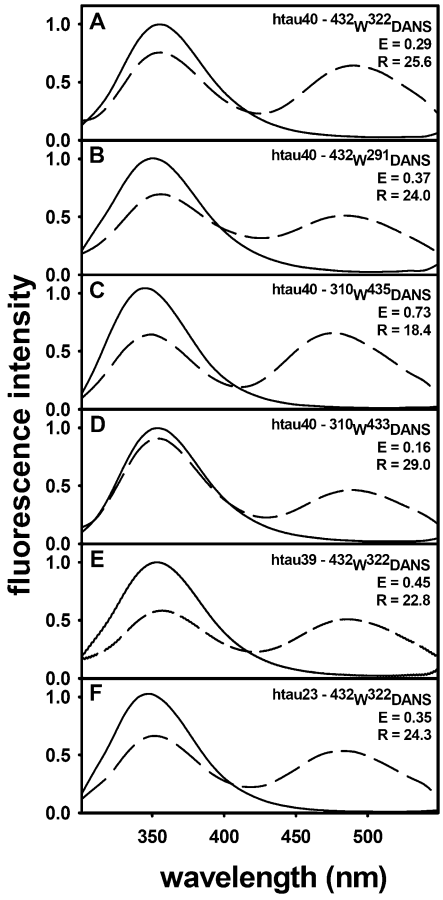

FIGURE 4: FRET between the repeat domain and the C-terminal domain. The fluorescence emission spectra are shown for htau40-432_W322_{DANS} (A), htau40-432_W291_{DANS} (B), htau40-310_W435_{DANS} (C), htau40-310_W433_{DANS} (D), htau39-432_W322_{DANS} (E), and htau23-432_W322_{DANS} (F). Experimental conditions were as described in the legend of Figure 3.

the case of unfolded proteins (*38*). For 12 or 19 amino acids, the mean distance in a random coil structure would be calculated to be 28 or 36 Å, respectively. The observed FRET distances of ~20 Å are smaller, arguing that the assumption of a pure random coil is not applicable and that a residual structure is adopted by the repeat domain, at least in the second and third repeats (see the Discussion).

In the experiments described above and the subsequent ones, there was a concern that the observed FRET might, in part, arise from intermolecular effects, rather than intramolecular effects due to folding. This possibility was, however, excluded by titration experiments. First, the labeled protein was titrated with an excess of nonfluorescent protein, htau40wt which has no tryptophan, which did not affect FRET efficiency. The same was found when we titrated labeled protein either with tryptophan containing htau40 or with labeled protein. In all cases, the data were consistent with intramolecular FRET only (data not shown).

Interaction of the C-Terminal Tail and the Repeat Domain. The distance between the repeat region and the C-terminal tail was analyzed by FRET using mutants carrying W310 and IAEDANS at position 435 or 433 in the htau40 isoform and vice versa with tryptophan at position 432 and IAEDANS at position 291 or 322 in tau40, htau39, and htau23 isoforms (Figure 4A−D). The FRET analysis of htau40-432_W322_{DANS} (Figure 4A) and htau40-432_W291_{DANS} (Figure 4B) yielded

Table 1: Summary of Results[a]

isoform	W position	IAEDANS position	E_{FRET}	R (Å)	L (Å)	E_{DENAT}	R_{DENAT} (Å)
htau39	310	322	0.67	19.5	29.0		
htau40	310	322	0.67	19.5	29.0		
htau40	310	291	0.53	21.6	36.5	0.32	25.5
htau40	432	322	0.29	25.6	87.7		
htau40	432	291	0.37	24.0	99.3	0.08	32.7
htau40	310	435	0.73	18.4	93.5		
htau40	310	433	0.16	29.0	92.8		
htau39	432	322	0.45	22.8	87.7		
htau23	432	322	0.35	24.3	87.7		
htau40	18	322	0.14	30.1	138.1	0.09	32.3
htau40	18	291	0.08	33.5	145.9		
htau40	310	17	0.19	28.0	143.2		
htau39	18	322	0.18	28.8	138.1		
htau23	18	322	0.19	27.8	122.7		
htau40	432	17	0.59	20.8	170.4		
htau23	432	17	0.36	24.2	151.1		

[a] FRET efficiencies (E_{FRET}), FRET distances (R), and theoretical distances (L) are given for various mutants on the basis of htau40, htau39, and htau23. For some mutants, the observed distances after chemical denaturation (R_{DENAT}) are also listed.

efficiencies of 0.29 and 0.37, respectively, corresponding to distances of 25.6 and 24 Å, respectively (see also Table 1). These distances are surprisingly short, considering that the FRET pairs are more than 100 residues apart in the polypeptide chain. The theoretical predictions for a random coil model between the 291 and 432 and 322 and 432 pairs are 99.3 and 87.7 Å, respectively, ~4 times larger than the observed distances. The color-swapped FRET pair in the mutant htau40-310_W435_{DANS} (Figure 4C) exhibited an even higher efficiency ($E = 0.73$) and a resulting distance of only 18.4 Å.

In contrast, another mutant with the IAEDANS label at residue 433, only two residues upstream of the previous position (htau40-310_W433_{DANS}, Figure 4D), yielded a very low efficiency of 0.16, corresponding to a distance of 29 Å. This remarkable decrease in the magnitude of the FRET signal within two residues (from the 435 and 310 pair to the 433 and 310 pair) cannot be explained simply by distance considerations alone. A more likely interpretation is a conformational change in the C-terminal tail which may fold over the repeat domain in one labeled mutant but not in the other [note that the tail may adopt an α-helical structure (*25*, *30*), and see the Discussion].

The mutant htau39-432_W322_{DANS} based on the isoform htau39 exhibited a similar efficiency ($E = 0.45$) with a calculated distance of 22.8 Å (Figure 4E). Thus, the missing second repeat in htau39 (upstream of the reporter W310) does not affect FRET between the C-terminus and the third repeat. The same was true for the mutant of htau23 (htau23-432_W322_{DANS}, Figure 4F), which showed an efficiency of 0.35 and a resulting distance of 24.3 Å. Thus, the absence of the N-terminal inserts has no impact on the interaction between the C-terminal end of tau and the center of the repeat domain either.

FRET Shows that the N-Terminus and the Repeat Domain Stay Apart. The interaction of the repeat region and the N-terminal end of tau was analyzed with mutants of htau40, htau39, and htau23 isoforms containing 18W and IAEDANS at position 291 or 322 and also a htau40 mutant with 310W and IAEDANS at position 17. In all cases, the FRET

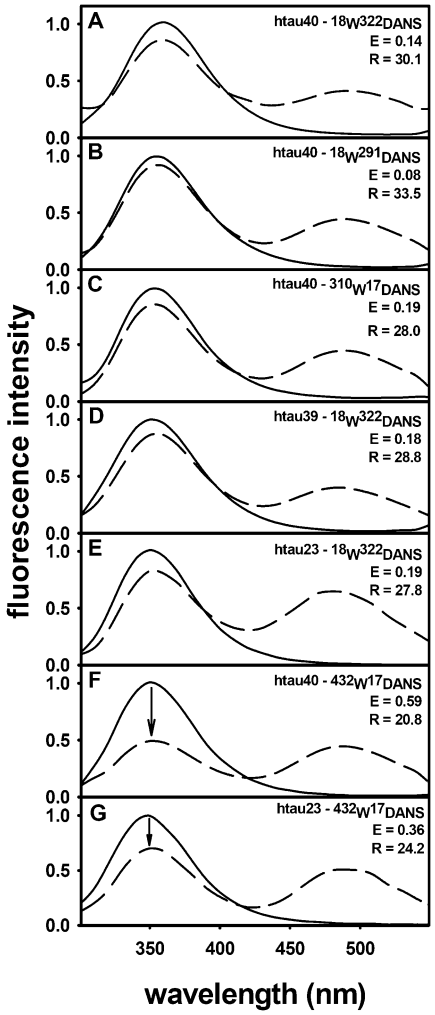

FIGURE 5: FRET between the repeat domain and the N-terminus and between the N-terminal and C-terminal domains. The fluorescence emission spectra are shown for htau40-18_W322_{DANS} (A), htau40-18_W291_{DANS} (B), htau40-310_W17_{DANS} (C), htau39-18_W322_{DANS} (D), htau23-18_W322_{DANS} (E), htau40-432_W17_{DANS} (F), and htau23-432_W17_{DANS} (G). Experimental conditions were as described in the legend of Figure 3. Note the pronounced FRET between the C-terminal and N-terminal domains (arrows in panels F and G).

efficiency was low (Figure 5A−E). For htau40-18_W322_{DANS} and htau40-18_W291_{DANS}, the observed FRET efficiencies were 0.14 and 0.08, respectively, resulting in distances of 30.1 and 33.5 Å, respectively (Figure 5A,B).

Likewise, for the dye-swapped mutant, htau40-310_W17_{DANS}, the efficiency was 0.19 and the corresponding distance was calculated to be 28 Å (Figure 5C). Similar results were obtained for the three-repeat isoforms htau39 and htau23. The efficiency for htau39-18_W322_{DANS} (Figure 5D) was 0.18, corresponding to an R of 28.8 Å. For the shortest isoform htau23 mutant (htau23-18_W322_{DANS}), the FRET efficiency was 0.19, resulting in an R of 27.8 Å (Figure 5E). Thus, the FRET efficiencies are much lower than those between the C-terminus and repeats. In fact, the efficiencies below 0.2 are too small to allow a reliable determination of distances.

Short Distance between the Two Ends of Tau. To cover the largest possible distance within tau, we analyzed FRET between the N- and C-terminal domains in the mutant htau40-432_W17_{DANS} (Figure 5F). Interestingly, the observed efficiency was relatively high (0.59), resulting in a distance

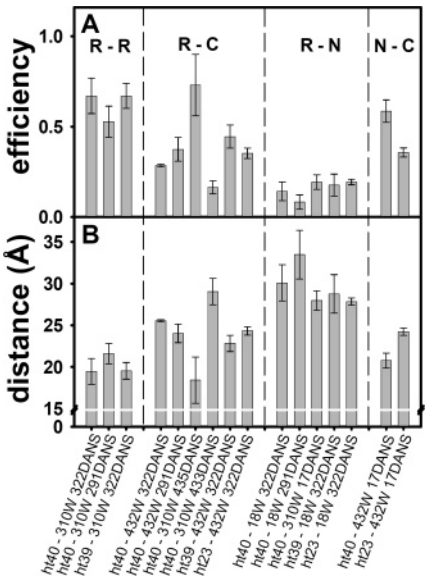

FIGURE 6: Summary of FRET efficiencies and calculated distances. The FRET efficiencies are summarized in panel A, and the resulting distances are given in angstroms in panel B. The different mutants are indicated below the diagram and are divided into four groups: R−R (FRET within the repeat region), R−C (FRET between the repeats and the C-terminus), R−N (FRET between the N-terminus and the repeat domain), and N−C (FRET between the N- and C-termini).

between the termini of 20.8 Å. This distance is much shorter than the theoretical value of 170 Å. A similar result was obtained with the mutant htau23-432_W17_{DANS}, yielding a FRET efficiency of 0.36 and a calculated distance of 24.2 Å (Figure 5G). Given the previous results that the N-terminus does not show FRET with the second or third repeat whereas the C-terminus does, and the observation that the ends of tau approach each other, the data suggest a complex of both termini and the repeats, mediated by the C-terminus of tau (see the Discussion).

The results of the FRET experiments are summarized in Figure 6. The efficiencies of FRET pairs within the repeats are between 0.53 and 0.67 (Figure 6, column R−R), resulting in distances of ∼20 Å. FRET between the C-terminus and the repeat domain exhibited a higher variability in efficiency, for example, when the IAEDANS label was located in the C-terminal tail, showing efficiencies between 0.16 (htau40-310_W433_{DANS}) and 0.73 (htau40-310_W435_{DANS}) (Figure 6, column R−C). This inconsistency points to a sequence dependence of the FRET efficiency in the C-terminal tail which might be caused by an effect of the IAEDANS label on the local secondary structure. In the dye swap mutant containing W in the C-terminus and IAEDANS in the repeats, this effect was not found. Overall, the efficiencies were ∼0.4, with a remarkable similarity between all isoforms, corresponding to distances of 23−25 Å between the C-terminus and the repeats. A similar coherent picture emerges for the different isoforms with regard to the distances between the N-terminus and the repeats (Figure 6, column R−N); all mutants exhibit a weak FRET signal with transfer efficiencies between 0.1 (htau40-18_W291_{DANS}) and 0.19 (htau40-310_W17_{DANS}), resulting in distances of 28−34 Å. The FRET efficiencies between the two ends of tau lie between 0.36 and 0.5 and are remarkably high, corresponding to distances of 21−24 Å (Figure 6, column N−C) which is much lower than the theoretical distance of 170 Å.

EPR Studies Confirm a Highly Flexible Structure along the Tau Chain. If the polypeptide chain of tau is internally folded, one might expect partial immobilization of residues. This question was addressed by EPR. Mutants of htau40-310_W with Cys at positions 17, 291, 322, and 431 were labeled with iodoacetamide spin-labels (JAA6) with a six-membered nitroxide ring (TEMPO, 2,2,6,6-tetramethyl-1-piperidine-*n*-oxyl). The EPR spectra provide information about the local secondary and tertiary structure and about the mobility of the spin-label. For example, highly mobile spin-label side chains yield three sharp lines similar in height and small line widths, but the width, shape, and height ratios of the absorption lines change when the motion becomes restricted (*43*, *44*). A quantitative measure of spin-label dynamics is the effective reorientational correlation time, τ_R, of the nitroxide which is determined by simulated spectra. Approximate values of τ_R can be calculated from the line width of the center line, ΔB_0, and the h_i/h_j line height ratios of the three lines (*45*).

The shapes of the EPR spectra of htau40-17_{JAA6}, htau40-431_{JAA6}, htau40-322_{JAA6}, and htau40-291_{JAA6} were similar (Figure 7A) and were indicative of a high flexibility, similar to that observed in flexible termini, flexible loop regions, or unstructured proteins (*43*). This agrees well with recent observations on the mobility of residues in the third repeat (*46*). Detailed comparison of the high-field lines (Figure 7B) revealed small differences between the spectra of labeled mutants, indicating that the C-terminal domain (JAA6 at residue 431) has the highest mobility, followed by the repeat (JAA6 at residues 291 and 322) and the N-terminal domain (JAA6 at residue 17). The spin-label mobility was expressed in terms of the effective rotational correlation times of the four investigated mutants and an unbound spin-label for comparison (Figure 7C). The rotational correlation time of htau40-17_{JAA6} was the highest (∼0.6 ns), whereas the mutants with the spin-label within the repeat region (htau40-291_{JAA6} and htau40-322_{JAA6}) exhibited rotational correlation times of ∼0.4 ns. The lowest correlation time and therefore the highest mobility were found for htau40-431_{JAA6} (∼0.2 ns). For comparison, the correlation time of an unbound TEMPO label (2,2,6,6-tetramethyl-1-piperidine-*n*-oxyl) was ∼0.05 ns, whereas that of a label immobilized inside a well-folded protein is typically 2 orders of magnitude higher (*47*).

Denaturation of Tau Increases the Stokes Radius and Decreases FRET Efficiencies. The distance between the C-terminus and the repeat domain and between the two ends of tau pointed to a residual structure within a mostly unfolded protein. This fact raised the question of the stability of the interaction. This was probed by assessing FRET in the presence of increasing concentrations of the denaturant GdnHCl. In addition, to check the influence of GdnHCl on the overall size of the tau molecules, we analyzed their Stokes radii by size exclusion chromatography (Figure 8A). All six naturally occurring isoforms and the constructs K19 and K18 comprising three or four repeats were analyzed in PBS with up to 2 M GdnHCl. Without a denaturant, the correlation

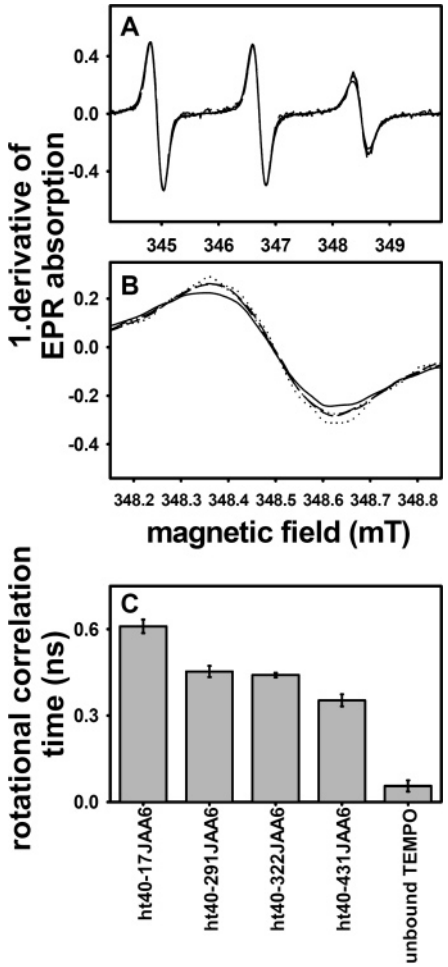

FIGURE 7: Electron paramagnetic resonance spectroscopy. X-Band EPR spectra of htau40-17$_{JAA6}$, htau40-291$_{JAA6}$, htau40-322$_{JAA6}$, and htau40-431$_{JAA6}$ are shown in panel A. Small differences in the high-field peak indicate also slight differences in label mobility (see panel B for details). The spectra of the high-field peak are shown for htau40-17$_{JAA6}$ (—), htau40-431$_{JAA6}$ (– – –), htau40-322$_{JAA6}$ (- - -), and htau40-291$_{JAA6}$ (•••). Differences in the high-field peak of the EPR spectra show significant differences in label mobility at the C- and N-termini, whereas the mobilities in the repeat region were almost identical. The corresponding rotational correlation time (C) is a measure for the immobility of the TEMPO label. For comparison, the unbound TEMPO is also shown (C). Error bars indicate the doubled standard error.

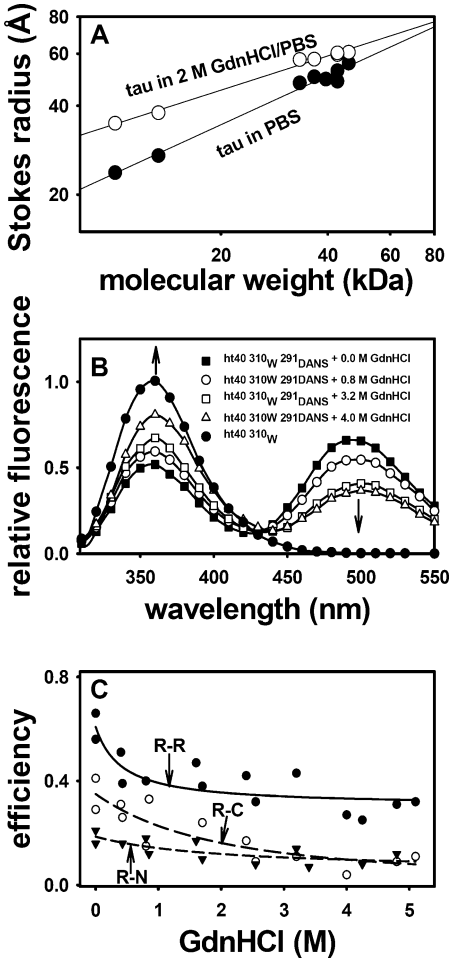

FIGURE 8: Denaturation of tau destroys folding and inhibits FRET. Tau isoforms and constructs comprising three or four repeats were analyzed by size exclusion chromatography in the absence (●) and presence (○) of 2 M GdnHCl. (A) Stokes radii of natively unfolded tau are calculated by reference to a standard of globular proteins and plotted vs their molecular weights. Note the increase in the Stokes radius upon exposure to the denaturant. (B) Fluorescence of htau40-310$_W$291$_{DANS}$ with increasing concentrations of GdnHCl shows a decreasing FRET efficiency; i.e., the magnitude of the tryptophan peak increases, and concomitantly, the magnitude of the IAEDANS peak decreases (arrows). (C) Summary of other FRET pairs (R−R, htau40-310$_W$291$_{DANS}$; R−C, htau40-432$_W$-291$_{DANS}$; and R−N, htau40-18$_W$322$_{DANS}$) measured in the presence of increasing GdnHCl concentrations. FRET efficiencies are plotted vs GdnHCl concentration.

between the Stokes radius and the molecular weight corresponded to that expected for natively unfolded proteins (*18*, *48*). After incubation with 2 M GdnHCl, the Stokes radii increased to values expected for fully denatured proteins (*49*). Thus, even though tau behaves as a natively unfolded protein in physiological buffers, the peptide chain could be further expanded by denaturation in GdnHCl.

We therefore asked what consequences the denaturation would have on the FRET efficiencies between FRET pairs. For example, htau40-310$_W$291$_{DANS}$ (Figure 8B) showed an increasing tryptophan peak and a decreasing peak of IAEDANS at increasing concentrations of GdnHCl (0−5 M), consistent with a lower FRET efficiency. The same experiments were performed with htau40-432$_W$291$_{DANS}$ and htau40-18$_W$322$_{DANS}$, and the FRET efficiencies were plotted versus the concentration of GdnHCl (Figure 8C). In the case of htau40-310$_W$291$_{DANS}$, the FRET efficiency dropped from 0.53 to 0.32. Thus, this FRET pair undergoes a significant change but retains a reasonable FRET efficiency which allows a reliable determination of distance which changes from 21.6 to 25.5 Å at 5 M GdnHCl. This distance is still shorter than the theoretical distance of 36.5 Å, but with regard to the uncertainty of theoretical distances in random coil structures, it is still within a reasonable range. For the distance between the repeats and the C-terminus (htau40-432$_W$291$_{DANS}$), the FRET efficiency dropped from ∼0.3 to <0.1, which makes it difficult to calculate reliable distances. The situation is different for FRET between the N-terminal and repeat domains. In the case of htau40-18$_W$322$_{DANS}$, there is very little FRET in the soluble state (0.14) and this decreases even further to 0.1. In summary, FRET within the repeats can be inhibited by GdnHCl but remains measurable, whereas FRET between the two termini and the repeats disappears almost completely.

DISCUSSION

The aim of this study was to obtain information about the global conformation of tau protein in solution. Tau is interesting from three perspectives. (1) It is important for the cell biology of the neurons because it stabilizes microtubules for their role in neurite outgrowth and axonal transport. (2) Its pathological aggregation in neurons constitutes one of the hallmarks of Alzheimer's disease. (3) Tau belongs to the growing class of natively unfolded proteins which display novel features in protein chemistry.

Precise structural information about tau in solution has been difficult to obtain since its lack of defined structure precludes a crystallographic analysis. Spectroscopic evidence (CD, FTIR, and fluorescence), solution X-ray scattering, and hydrodynamic evidence highlight the natively unfolded character of the protein, characterized by a lack of secondary structure, Gaussian coil-type character with a persistence length of ~2 nm, and an unusually large volume (*6*, *7*, *18*, *40*). Electron microscopy reveals that under certain conditions tau can adopt a rather extended form and has a tendency to dimerize (*5*). When bound to microtubules, tau tends to align along the protofilament ridges but retains much of its disordered state (*50*, *51*). NMR spectroscopy confirms the paucity of secondary structure but, in addition, highlights certain sequence motifs with an enhanced propensity for β-structure which are known to play a role in the abnormal aggregation to Alzheimer PHFs (*52*, *53*) [note that several other NMR studies have reported on the structure of tau-derived peptides (*54*, *55*), but since these studies were performed in structure-inducing buffers, their significance remains debatable].

On the other hand, other indirect observations suggest that tau cannot simply be a total random coil. Although tau is largely unfolded, it retains some inherent structure which can be destroyed by denaturation. The repeat domain of tau represents the core of the microtubule binding and PHF aggregating function of tau and is enriched with β-forming elements (*56*). Perhaps the most compelling hints for conformational states come from the reactivities of antibodies with discontinuous epitopes which often recognize tau at an early stage of neurodegeneration. Examples are the Alz50 and MC1 antibodies which recognize an epitope formed by residues near the N-terminus (residues 7−9) and residues in the third repeat (313−322) (*31*, *32*, *57*), antibody Tau-66 which recognizes elements upstream of the repeat domain and residues in repeat R3 (*58*, *59*), antibody MN423 which reacts against a truncation site downstream of the repeats (at E391) and residues within the repeat domain (*60*), and antibody SMI34 which reacts with an epitope that requires the repeat domain and one of the KSP motifs upstream or downstream from the repeats (*61*). These observations are in good agreement with these results and are suggestive of a global folding back of N- or C-terminal domains over the repeat domain which is transient in soluble tau but may become more stable (and thus detectable by antibodies) in pathologically folded tau. Similar conclusions are echoed by the distribution of tau mutations found in frontotemporal dementias (FTDP-17). Most of them occur in or near the repeat domain, consistent with the fact that this domain is responsible for microtubule binding and PHF assembly (*62*). However, some mutations lie toward the ends of the tau molecule, e.g., R5L or R406W, compatible with the idea of a global hairpin folding of tau. This is now confirmed and placed on a more quantitative basis by the data reported here. The main results follow.

(1) In solution, the intrarepeat distances from residue 310 to 322 or from residue 310 to 291 are short (~20 Å) and therefore show pronounced FRET, consistent with some local compaction due to folding.

(2) The C-terminal domain (residues 432 and 435) is much closer (19−23 Å) to the center of the repeats (residues 291, 310, and 322) than expected, giving rise to substantial FRET and suggesting a hairpinlike folding back of the tail onto the repeats.

(3) The N-terminal domain (residue 17) is not within FRET range of the repeat domain, but it is close to the C-terminal end (21−24 Å).

By denaturation, one would expect a significant change in the distances of the FRET pairs which are widely separated along the protein sequence. In fact, the distances we observed do not show the full effect. In the case of the intrarepeat FRET pair (291−310), the distance increased from the native state of 21 Å to an apparent distance of 26 Å, whereas the theoretical model expects 36 Å for a random coil. This can be explained by noting that neither the initial state nor the chemically denatured state may comply with the assumptions about standard protein structure, which was also found by denaturing well-folded proteins (*63*, *64*). The initial state of a folded protein has a sharply defined distance distribution between a given pair of residues whose FRET efficiency can be translated into a well-defined separation. This does not necessarily hold for a natively unfolded protein such as tau which exists in solution as a mixture of random coil, residual secondary structure elements, and preferred conformational states which are moreover heterogeneous and mobile (as evidenced by the EPR data here). In mostly unfolded proteins, the distance between a given FRET pair shows a wider distribution and the apparent FRET reflects this heterogeneity (*65*). On the other hand, the chemically denatured state may differ significantly from a pure random coil model (*66*), especially in the presence of pronounced charge asymmetries (as is the case with tau).

Together, these data show that tau in solution is globally folded in a double sense, reminiscent of a paperclip, as depicted in Figure 9. Both the C- and N-termini must be folded over to be near the center of the repeat domain. Several lines of evidence argue that the global folding is specific but rather weak. First, "dye-swapped" FRET pairs (exchange of the positions of Trp and the dansyl label) yield similar distances; second, the energy transfer can be largely disrupted by mild denaturation (~1 M GdnHCl), and third, for certain residues, the FRET effect becomes "forbidden", presumably because the insertion of a bulky label perturbs the conformation. This is illustrated by moving the label from residue 435 (strong FRET) to 433 (no FRET). The difference between these two positions can be explained by either a disruption of the local conformation which might be a prerequisite for interaction with the repeat region or a direct effect on interaction while the assumed local helical structure remains intact. We note that this region is predicted to be an amphipathic α-helix (*25*), and therefore, a change by two residues could easily convert an allowed label position into a forbidden one.

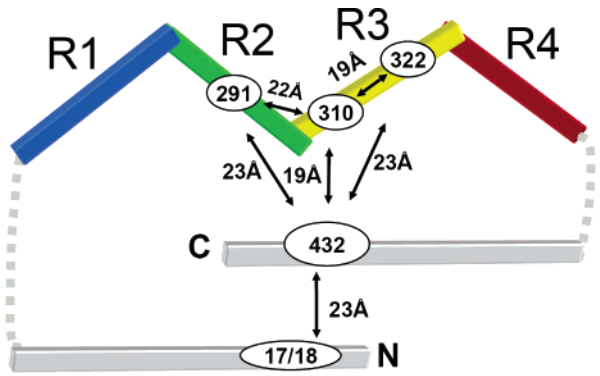

FIGURE 9: Model of intramolecular interactions within soluble tau. The polypeptide chain of a four-repeat tau (htau40) is shown with differently colored repeats (R1 in blue, R2 in green, R3 in yellow, and R4 in red) and the adjacent N- and C-terminal sequences in gray. The positions of FRET partners are indicated. They lie near the N-terminus (residue 17 or 18), near the C-terminus (residue 432 or 435), and in the repeat domain [residue 291 in the second repeat (green) and residues 310 and 322 in the third repeat (yellow)]. The C-terminus folds in the vicinity of the repeat domain as well as the N-terminus, whereas the N-terminus stays beyond the FRET distance of the repeats.

One might expect that the end-to-end and end-to-center interactions within tau might cause some stabilization of the chain against fluctuations. To check this, we placed spin-labels in various positions. Although some differences were observed, the mobility remained very high, close to the value of denatured proteins. This reinforces the view that the folding interactions are short-lived and do not have the character of a firm docking of two binding sites that would cause substantial immobilization.

In summary, despite its natively unfolded character, the tau molecule possesses a paperclip-like suprastructure in solution whereby the two ends of the molecule approach each other and the repeat domain. This interaction is fluctuating, imposed on a chain that otherwise is almost as flexible as a denatured protein. This folding agrees well with the reactivities of certain antibodies (Alz50, MC1, Tau66, and SMI34) that detect abnormal tau in early stages of Alzheimer's disease, suggesting that a stabilization of the folded state could have pathological consequences. The approach presented here opens the path to analysis of the effect of phosphorylation, which causes an upshift in SDS−PAGE (*33*) and is held responsible for early changes in the conformation of tau in AD (*67*). Whether the suprastructure is retained in the microtubule-bound or PHF-aggregated state of tau is not known and is under investigation.

ACKNOWLEDGMENT

We are grateful to Dr. Eva-Maria Mandelkow for advice throughout the project, Dr. Jacek Biernat for help with all issues regarding cloning, and Dr. Alexander Marx for fruitful discussions about protein conformation. We also thank Bianca Wichmann for excellent technical assistance.

REFERENCES

1. Garcia, M. L., and Cleveland, D. W. (2001) Going new places using an old MAP: Tau, microtubules and human neurodegenerative disease, *Curr. Opin. Cell Biol. 13*, 41−8.
2. Gamblin, T. C., Berry, R. W., and Binder, L. I. (2003) Modeling tau polymerization in vitro: A review and synthesis, *Biochemistry 42*, 15009−17.
3. Lee, V. M., Goedert, M., and Trojanowski, J. Q. (2001) Neurodegenerative tauopathies, *Annu. Rev. Neurosci. 24*, 1121−59.
4. Cleveland, D. W., Hwo, S. Y., and Kirschner, M. W. (1977) Physical and chemical properties of purified tau factor and the role of tau in microtubule assembly, *J. Mol. Biol. 116*, 227−47.
5. Wille, H., Drewes, G., Biernat, J., Mandelkow, E. M., and Mandelkow, E. (1992) Alzheimer-like paired helical filaments and antiparallel dimers formed from microtubule-associated protein tau in vitro, *J. Cell Biol. 118*, 573−84.
6. Schweers, O., Schonbrunn-Hanebeck, E., Marx, A., and Mandelkow, E. (1994) Structural studies of tau protein and Alzheimer paired helical filaments show no evidence for β-structure, *J. Biol. Chem. 269*, 24290−7.
7. von Bergen, M., Friedhoff, P., Biernat, J., Heberle, J., Mandelkow, E. M., and Mandelkow, E. (2000) Assembly of tau protein into Alzheimer paired helical filaments depends on a local sequence motif ((306)VQIVYK(311)) forming β structure, *Proc. Natl. Acad. Sci. U.S.A. 97*, 5129−34.
8. Barghorn, S., and Mandelkow, E. (2002) Toward a unified scheme for the aggregation of tau into Alzheimer paired helical filaments, *Biochemistry 41*, 14885−96.
9. Chen, J., Kanai, Y., Cowan, N. J., and Hirokawa, N. (1992) Projection domains of MAP2 and tau determine spacings between microtubules in dendrites and axons, *Nature 360*, 674−7.
10. Butner, K. A., and Kirschner, M. W. (1991) Tau protein binds to microtubules through a flexible array of distributed weak sites, *J. Cell Biol. 115*, 717−30.
11. Gustke, N., Trinczek, B., Biernat, J., Mandelkow, E. M., and Mandelkow, E. (1994) Domains of tau protein and interactions with microtubules, *Biochemistry 33*, 9511−22.
12. Goode, B. L., Denis, P. E., Panda, D., Radeke, M. J., Miller, H. P., Wilson, L., and Feinstein, S. C. (1997) Functional interactions between the proline-rich and repeat regions of tau enhance microtubule binding and assembly, *Mol. Biol. Cell 8*, 353−65.
13. Levy, S. F., Leboeuf, A. C., Massie, M. R., Jordan, M. A., Wilson, L., and Feinstein, S. C. (2005) Three- and four-repeat tau regulate the dynamic instability of two distinct microtubule subpopulations in qualitatively different manners. Implications for neurodegeneration, *J. Biol. Chem. 280*, 13520−8.
14. Wischik, C. M., Novak, M., Edwards, P. C., Klug, A., Tichelaar, W., and Crowther, R. A. (1988) Structural characterization of the core of the paired helical filament of Alzheimer disease, *Proc. Natl. Acad. Sci. U.S.A. 85*, 4884−8.
15. Jakes, R., Novak, M., Davison, M., and Wischik, C. M. (1991) Identification of 3- and 4-repeat tau isoforms within the PHF in Alzheimer's disease, *EMBO J. 10*, 2725−9.
16. Friedhoff, P., Schneider, A., Mandelkow, E. M., and Mandelkow, E. (1998) Rapid assembly of Alzheimer-like paired helical filaments from microtubule-associated protein tau monitored by fluorescence in solution, *Biochemistry 37*, 10223−30.
17. von Bergen, M., Barghorn, S., Li, L., Marx, A., Biernat, J., Mandelkow, E. M., and Mandelkow, E. (2001) Mutations of tau protein in frontotemporal dementia promote aggregation of paired helical filaments by enhancing local β-structure, *J. Biol. Chem. 276*, 48165−74.
18. Barghorn, S., Davies, P., and Mandelkow, E. (2004) Tau paired helical filaments from Alzheimer's disease brain and assembled in vitro are based on β-structure in the core domain, *Biochemistry 43*, 1694−703.
19. Novak, M., Kabat, J., and Wischik, C. M. (1993) Molecular characterization of the minimal protease resistant tau-unit of the Alzheimer's-disease paired helical filament, *EMBO J. 12*, 365−70.
20. Rissman, R. A., Poon, W. W., Blurton-Jones, M., Oddo, S., Torp, R., Vitek, M. P., LaFerla, F. M., Rohn, T. T., and Cotman, C. W. (2004) Caspase-cleavage of tau is an early event in Alzheimer disease tangle pathology, *J. Clin. Invest. 114*, 121−30.
21. Gamblin, T. C., Chen, F., Zambrano, A., Abraha, A., Lagalwar, S., Guillozet, A. L., Lu, M., Fu, Y., Garcia-Sierra, F., LaPointe, N., Miller, R., Berry, R. W., Binder, L. I., and Cryns, V. L. (2003) Caspase cleavage of tau: Linking amyloid and neurofibrillary tangles in Alzheimer's disease, *Proc. Natl. Acad. Sci. U.S.A. 100*, 10032−7.
22. Goedert, M., Jakes, R., Spillantini, M. G., Hasegawa, M., Smith, M. J., and Crowther, R. A. (1996) Assembly of microtubule-associated protein tau into Alzheimer-like filaments induced by sulphated glycosaminoglycans, *Nature 383*, 550−3.
23. Kampers, T., Friedhoff, P., Biernat, J., Mandelkow, E. M., and Mandelkow, E. (1996) RNA stimulates aggregation of microtu-

bule-associated protein tau into Alzheimer-like paired helical filaments, *FEBS Lett. 399*, 344−9.
24. Abraha, A., Ghoshal, N., Gamblin, T. C., Cryns, V., Berry, R. W., Kuret, J., and Binder, L. I. (2000) C-Terminal inhibition of tau assembly in vitro and in Alzheimer's disease, *J. Cell Sci. 113* (Part 21), 3737−45.
25. Berry, R. W., Abraha, A., Lagalwar, S., LaPointe, N., Gamblin, T. C., Cryns, V. L., and Binder, L. I. (2003) Inhibition of tau polymerization by its carboxy-terminal caspase cleavage fragment, *Biochemistry 42*, 8325−31.
26. Harada, A., Oguchi, K., Okabe, S., Kuno, J., Terada, S., Ohshima, T., Sato-Yoshitake, R., Takei, Y., Noda, T., and Hirokawa, N. (1994) Altered microtubule organization in small-calibre axons of mice lacking tau protein, *Nature 369*, 488−91.
27. Brandt, R., Leger, J., and Lee, G. (1995) Interaction of tau with the neural plasma membrane mediated by tau's amino-terminal projection domain, *J. Cell Biol. 131*, 1327−40.
28. Sontag, E., Nunbhakdi-Craig, V., Lee, G., Brandt, R., Kamibayashi, C., Kuret, J., White, C. L., III, Mumby, M. C., and Bloom, G. S. (1999) Molecular interactions among protein phosphatase 2A, tau, and microtubules. Implications for the regulation of tau phosphorylation and the development of tauopathies, *J. Biol. Chem. 274*, 25490−8.
29. Mandelkow, E. M., and Mandelkow, E. (1998) Tau in Alzheimer's disease, *Trends Cell Biol. 8*, 425−7.
30. Gamblin, T. C., Berry, R. W., and Binder, L. I. (2003) Tau polymerization: Role of the amino terminus, *Biochemistry 42*, 2252−7.
31. Jicha, G. A., Bowser, R., Kazam, I. G., and Davies, P. (1997) Alz-50 and MC-1, a new monoclonal antibody raised to paired helical filaments, recognize conformational epitopes on recombinant tau, *J. Neurosci. Res. 48*, 128−32.
32. Carmel, G., Mager, E. M., Binder, L. I., and Kuret, J. (1996) The structural basis of monoclonal-antibody Alz50s selectivity for Alzheimer's-disease pathology, *J. Biol. Chem. 271*, 32789−95.
33. Biernat, J., Mandelkow, E. M., Schroter, C., Lichtenberg-Kraag, B., Steiner, B., Berling, B., Meyer, H., Mercken, M., Vandermeeren, A., Goedert, M., et al. (1992) The switch of tau protein to an Alzheimer-like state includes the phosphorylation of two serine-proline motifs upstream of the microtubule binding region, *EMBO J. 11*, 1593−7.
34. Hudson, E. N., and Weber, G. (1973) Synthesis and characterization of two fluorescent sulfhydryl reagents, *Biochemistry 12*, 4154−61.
35. Li, G., Levitus, M., Bustamante, C., and Widom, J. (2005) Rapid spontaneous accessibility of nucleosomal DNA, *Nat. Struct. Mol. Biol. 12*, 46−53.
36. Wu, P., and Brand, L. (1994) Conformational flexibility in a staphylococcal nuclease mutant K45C from time-resolved resonance energy transfer measurements, *Biochemistry 33*, 10457−62.
37. Matsumoto, S., and Hammes, G. G. (1975) Fluorescence energy transfer between ligand binding sites on aspartate transcarbamylase, *Biochemistry 14*, 214−24.
38. Fitzkee, N. C., and Rose, G. D. (2004) Reassessing random-coil statistics in unfolded proteins, *Proc. Natl. Acad. Sci. U.S.A. 101*, 12497−502.
39. Goedert, M., Spillantini, M. G., Potier, M. C., Ulrich, J., and Crowther, R. A. (1989) Cloning and sequencing of the cDNA encoding an isoform of microtubule-associated protein tau containing four tandem repeats: Differential expression of tau protein mRNAs in human brain, *EMBO J. 8*, 393−9.
40. Li, L., von Bergen, M., Mandelkow, E. M., and Mandelkow, E. (2002) Structure, stability, and aggregation of paired helical filaments from tau protein and FTDP-17 mutants probed by tryptophan scanning mutagenesis, *J. Biol. Chem. 277*, 41390−400.
41. Makrides, V., Massie, M. R., Feinstein, S. C., and Lew, J. (2004) Evidence for two distinct binding sites for tau on microtubules, *Proc. Natl. Acad. Sci. U.S.A. 101*, 6746−51.
42. Eftink, M. R. (1991) Fluorescence techniques for studying protein structure, *Methods Biochem. Anal. 35*, 127−205.
43. Steinhoff, H. J. (2002) Methods for study of protein dynamics and protein−protein interaction in protein-ubiquitination by electron paramagnetic resonance spectroscopy, *Front Biosci. 7*, c97−110.
44. Hubbell, W. L., Cafiso, D. S., and Altenbach, C. (2000) Identifying conformational changes with site-directed spin labeling, *Nat. Struct. Biol. 7*, 735−9.
45. Lund, J., and Dalton, H. (1985) Further characterisation of the FAD and Fe2S2 redox centres of component C, the NADH: acceptor reductase of the soluble methane monooxygenase of *Methylococcus capsulatus* (Bath), *Eur. J. Biochem. 147*, 291−6.
46. Margittai, M., and Langen, R. (2004) Template-assisted filament growth by parallel stacking of tau, *Proc. Natl. Acad. Sci. U.S.A. 101*, 10278−83.
47. Steinhoff, H. J. (1990) Residual motion of hemoglobin-bound spin labels and protein dynamics: Viscosity dependence of the rotational correlation times, *Eur. Biophys. J. 18*, 57−62.
48. Tcherkasskaya, O., and Uversky, V. N. (2003) Polymeric aspects of protein folding: A brief overview, *Protein Pept. Lett. 10*, 239−45.
49. Uversky, V. N. (2002) Natively unfolded proteins: A point where biology waits for physics, *Protein Sci. 11*, 739−56.
50. Santarella, R. A., Skiniotis, G., Goldie, K. N., Tittmann, P., Gross, H., Mandelkow, E. M., Mandelkow, E., and Hoenger, A. (2004) Surface-decoration of microtubules by human tau, *J. Mol. Biol. 339*, 539−53.
51. Al-Bassam, J., Ozer, R. S., Safer, D., Halpain, S., and Milligan, R. A. (2002) MAP2 and tau bind longitudinally along the outer ridges of microtubule protofilaments, *J. Cell Biol. 157*, 1187−96.
52. Goux, W. J., Kopplin, L., Nguyen, A. D., Leak, K., Rutkofsky, M., Shanmuganandam, V. D., Sharma, D., Inouye, H., and Kirschner, D. A. (2004) The formation of straight and twisted filaments from short tau peptides, *J. Biol. Chem. 279*, 26868−75.
53. Mukrasch, M. D., Biernat, J., von Bergen, M., Griesinger, C., Mandelkow, E., and Zweckstetter, M. (2005) Sites of TAU important for aggregation populate β-structure and bind to microtubules and polyanions, *J. Biol. Chem.* (in press).
54. Minoura, K., Tomoo, K., Ishida, T., Hasegawa, H., Sasaki, M., and Taniguchi, T. (2002) Amphipathic helical behavior of the third repeat fragment in the tau microtubule-binding domain, studied by ^{1}H NMR spectroscopy, *Biochem. Biophys. Res. Commun. 294*, 210−4.
55. Minoura, K., Yao, T. M., Tomoo, K., Sumida, M., Sasaki, M., Taniguchi, T., and Ishida, T. (2004) Different associational and conformational behaviors between the second and third repeat fragments in the tau microtubule-binding domain, *Eur. J. Biochem. 271*, 545−52.
56. von Bergen, M., Barghorn, S., Biernat, J., Mandelkow, E. M., and Mandelkow, E. (2005) Tau aggregation is driven by a transition from random coil to β sheet structure, *Biochim. Biophys. Acta 1739*, 158−66.
57. Jicha, G. A., Lane, E., Vincent, I., Otvos, L., Jr., Hoffmann, R., and Davies, P. (1997) A conformation- and phosphorylation-dependent antibody recognizing the paired helical filaments of Alzheimer's disease, *J. Neurochem. 69*, 2087−95.
58. Ghoshal, N., Garcia-Sierra, F., Fu, Y., Beckett, L. A., Mufson, E. J., Kuret, J., Berry, R. W., and Binder, L. I. (2001) Tau-66: Evidence for a novel tau conformation in Alzheimer's disease, *J. Neurochem. 77*, 1372−85.
59. Garcia-Sierra, F., Ghoshal, N., Quinn, B., Berry, R. W., and Binder, L. I. (2003) Conformational changes and truncation of tau protein during tangle evolution in Alzheimer's disease, *J. Alzheimer's Dis. 5*, 65−77.
60. Skrabana, R., Kontsek, P., Mederlyova, A., Iqbal, K., and Novak, M. (2004) Folding of Alzheimer's core PHF subunit revealed by monoclonal antibody 423, *FEBS Lett. 568*, 178−82.
61. Lichtenberg-Kraag, B., Mandelkow, E. M., Biernat, J., Steiner, B., Schroter, C., Gustke, N., Meyer, H. E., and Mandelkow, E. (1992) Phosphorylation-dependent epitopes of neurofilament antibodies on tau protein and relationship with Alzheimer tau, *Proc. Natl. Acad. Sci. U.S.A. 89*, 5384−8.
62. Hutton, M. (2001) Missense and splice site mutations in tau associated with FTDP-17: Multiple pathogenic mechanisms, *Neurology 56*, S21−5.
63. Navon, A., Ittah, V., Scheraga, H. A., and Haas, E. (2002) Formation of the hydrophobic core of ribonuclease A through sequential coordinated conformational transitions, *Biochemistry 41*, 14225−31.

64. Krantz, B. A., Trivedi, A. D., Cunningham, K., Christensen, K. A., and Collier, R. J. (2004) Acid-induced unfolding of the amino-terminal domains of the lethal and edema factors of anthrax toxin, *J. Mol. Biol*. *344*, 739−56.

65. Schuler, B., Lipman, E. A., and Eaton, W. A. (2002) Probing the free-energy surface for protein folding with single-molecule fluorescence spectroscopy, *Nature 419*, 743−7.

66. Fitzkee, N. C., Fleming, P. J., Gong, H., Panasik, N., Jr., Street, T. O., and Rose, G. D. (2005) Are proteins made from a limited parts list? *Trends Biochem. Sci. 30*, 73−80.

67. Binder, L. I., Guillozet-Bongaarts, A. L., Garcia-Sierra, F., and Berry, R. W. (2005) Tau, tangles and Alzheimer's disease, *Biochim. Biophys. Acta 1739*, 216−23.

BI0521543